

# The effect of screening long-range Coulomb interactions on the metallic behavior in two-dimensional hole systems

L.H. Ho,<sup>1,2,\*</sup> W.R. Clarke,<sup>1</sup> A.P. Micolich,<sup>1</sup> R. Danneau,<sup>1,†</sup> O. Klochan,<sup>1</sup>  
M.Y. Simmons,<sup>1</sup> A.R. Hamilton,<sup>1,‡</sup> M. Pepper,<sup>3</sup> and D.A. Ritchie<sup>3</sup>

<sup>1</sup>*School of Physics, University of New South Wales, Sydney NSW 2052, Australia*

<sup>2</sup>*CSIRO Materials Science and Engineering, PO Box 218, Lindfield NSW 2070, Australia*

<sup>3</sup>*Cavendish Laboratory, University of Cambridge, Cambridge CB3 0HE, United Kingdom*

(Dated: October 26, 2018)

We have developed a technique utilizing a double quantum well heterostructure that allows us to study the effect of a nearby ground-plane on the metallic behavior in a GaAs two-dimensional hole system (2DHS) in a single sample and measurement cool-down, thereby maintaining a constant disorder potential. In contrast to recent measurements of the effect of ground-plane screening of the long-range Coulomb interaction in the insulating regime, we find surprisingly little effect on the metallic behavior when we change the distance between the 2DHS and the nearby ground-plane.

PACS numbers: 71.30.+h, 72.20.-i, 73.21.Fg

The ground state of a 2D electron or hole system is determined by the ratio  $r_s$  of the inter-particle Coulomb energy to the kinetic energy, with the regimes  $r_s \sim 0$ ,  $r_s \sim 10$ , and  $r_s \sim 100$  corresponding to the gas, liquid and solid phases of the 2D system. Recently, much effort has gone into studying the phase diagram of 2D systems, focussing on the role of interactions and disorder<sup>1</sup>. An interesting approach is to use an adjacent metallic ground-plane to screen the long-range Coulomb interactions, and thereby study how the length-scale of the Coulomb interactions controls the ground state of the 2D system. Ground-plane screening was used to probe the effect of Coulomb interactions in the melting of the Wigner crystal state of electrons on liquid helium<sup>2,3</sup>. More recently, Huang *et al.*<sup>4</sup> have used a nearby ground-plane to study the insulating state in an ultra-low density 2D hole system (2DHS), and find that the insulating behaviour is strongly affected by screening the Coulomb interaction. It would be interesting to perform a corresponding study for the metallic behavior observed in a dilute 2DHS. However, this presents a significant technical challenge because on one hand, the higher hole density  $p$  in the metallic regime requires that the distance  $d$  between the ground-plane and the 2DHS be quite small ( $d \sim 50$  nm) to achieve effective screening, and on the other, 2DHSs of sufficient quality to observe the metallic behavior are typically buried deep ( $> 100$  nm) in the semiconductor.

In this paper, we report a study of the influence of ground-plane screening on the metallic behavior in a 2DHS. We find that screening the long-range Coulomb interactions has a relatively small effect in the metallic regime, in contrast to the insulating behavior<sup>4</sup>. Our findings suggest that hole-hole screening within the 2DHS already significantly reduces long-range Coulomb interactions in the metallic regime, consistent with the view that the metallic behavior arises due to temperature-dependent screening of the Coulomb interactions between holes and charged impurities<sup>5,6,7</sup>. To overcome the technical challenge of studying the ground-plane screening

in the metallic regime, we have used a heterostructure featuring two quantum wells buried  $\sim 300$  nm beneath the semiconductor surface and separated by only 50 nm, such that the 2DHS in the upper quantum well acts as the nearby ground-plane for the 2DHS in the lower quantum well. Using a metal surface-gate, we can deplete the upper 2DHS, making the surface-gate become the ground-plane, and thus increasing the distance  $d$  to the ground-plane by a factor of  $\sim 7$ . This is a major advantage as  $d$  can be changed in a single device and measurement cool-down, thereby keeping the disorder relatively constant, unlike previous studies.

Our approach is illustrated in Fig. 1(a/b), and utilizes a double quantum well (DQW) structure featuring a doped semiconductor back-gate, an overall top-gate (TG) and a set of depletion gates (DG) adjacent to each AuBe ohmic contact. The top and back gates allow the hole densities  $p$  in the two 2DHSs to be controlled. The ohmic contacts connect to both QWs and the depletion gate is used to sever all connections to the upper 2DHS with the exception of the drain contact, via which the upper 2DHS is grounded (see Fig. 1(a)). Hence current passes only via the lower 2DHS. In this experiment, we measure the temperature dependent resistivity  $\rho(T)$  of the lower 2DHS when it is separated from a nearby ground plane by  $d = 50$  nm (Fig. 1(a)) and  $d = 340$  nm (Fig. 1(b)). For the  $d = 50$  nm case, the top-gate is set to 0 V, resulting in a 2DHS with a density of approximately  $1 \times 10^{11}$  cm<sup>-2</sup> in the upper QW, which acts as a ground plane. For the  $d = 340$  nm case, the top gate is set to  $\sim +0.35$  V, depleting the upper 2DHS in regions directly beneath the top gate. Despite being positively biased, the top-gate is still an equipotential, and hence acts as a ground-plane when the upper 2DHS is depleted. Combining this operating principle with appropriate adjustments to the various gate biases, we can switch between the two  $d$  values while keeping the density in the lower 2DHS constant, and repeat the experiment at different densities.

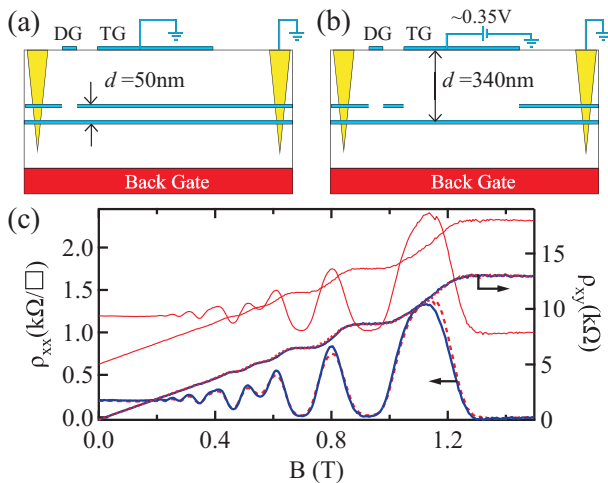


FIG. 1: (Color online) Schematic of the technique used to vary the distance  $d$  to the ground plane, where the upper 2DHS is (a) occupied ( $d = 50$  nm) or (b) depleted ( $d = 340$  nm). (c) A comparison of the longitudinal ( $\rho_{xx}$  - left axis) and Hall ( $\rho_{xy}$  - right axis) resistance of the lower 2DHS at  $p = 6.6 \times 10^{10} \text{ cm}^{-2}$  with  $V_{BG} = 0$  V for  $d = 340$  nm (solid blue lines) and  $d = 50$  nm (dashed red lines). The arrows indicate the relevant axes. The data for  $d = 50$  nm has been duplicated and offset upwards by  $1 \text{ k}\Omega/\square$  in  $\rho_{xx}$  and  $5 \text{ k}\Omega$  in  $\rho_{xy}$  (solid red lines) for clarity, since the data for the two  $d$  values overlap.

The device is fabricated on a (311)A AlGaAs/GaAs DQW heterostructure, featuring two 20nm GaAs QWs separated by a 30nm thick  $\text{Al}_{0.3}\text{Ga}_{0.7}\text{As}$  barrier that ensures there is no tunneling between the two 2DHSs ( $\Delta_{SAS} \ll 0.1$  K). The heavily-doped (311)A substrate acts as the back-gate and is separated by  $3 \mu\text{m}$  from the lower QW. The device is fabricated into a Hall bar structure oriented along the high-mobility [233] direction. Transport measurements were performed in a Kelvinox 100 dilution refrigerator, with a 20 mK base temperature. Standard four-terminal low-frequency a.c lock-in techniques were used with a constant excitation voltage of  $20 \mu\text{V}$  applied at  $f = 4$  Hz.

In Fig. 1(c) we present magnetotransport measurements in the two device configurations presented in Fig. 1 (a/b) to demonstrate that we can maintain a constant  $p$  in the lower 2DHS while changing the ground-plane distance from  $d = 50$  nm (dashed red trace) to  $d = 340$  nm (solid blue trace). Due to the close overlap of these two traces, we have reproduced the  $d = 50$  nm traces and offset them vertically for clarity (solid red lines). The Hall slope ( $\rho_{xy}$  - right axis) and the period of the Shubnikov-de Haas (SdH) oscillations ( $\rho_{xx}$  - left axis) show that the density remains constant to within 1% despite changing  $d$  by a factor of  $\sim 7$ .

We commence our study by comparing the temperature dependent resistivity  $\rho_{xx}(T)$  measured for  $d = 340$  nm with that obtained in a prior study using a similar p-GaAs heterostructure containing a single QW<sup>8</sup>. This allows us to confirm that the depleted upper 2DHS in our

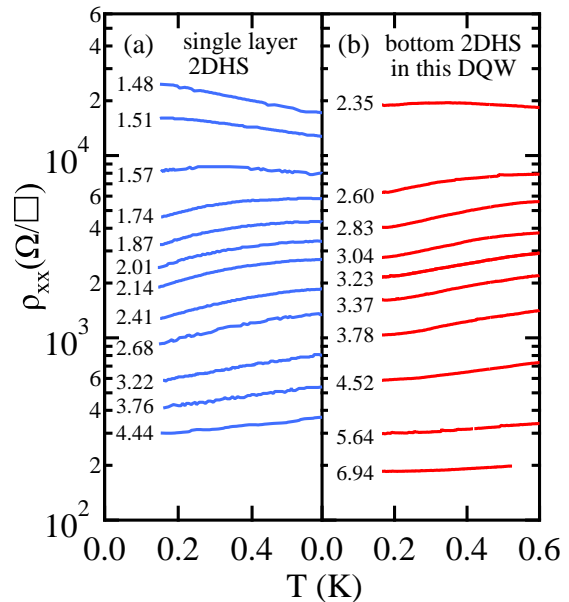


FIG. 2: (Color online) A comparison of the temperature dependent longitudinal resistivity  $\rho_{xx}(T)$  vs temperature  $T$  for: (a) a previously measured 2DHS in a similar single QW heterostructure<sup>8</sup>, and (b) the lower 2DHS of our device when the upper 2DHS is depleted ( $d = 340$  nm). The numbers beside each trace indicate the hole density in units of  $10^{10} \text{ cm}^{-2}$ .

device does not significantly alter the results obtained for large  $d$ . In Fig. 2(a) we show  $\rho_{xx}(T)$  data obtained in<sup>8</sup>, where a clear metal-insulator transition is observed. Insulating behavior ( $\frac{\partial \rho}{\partial T} < 0$ ) is observed at low densities, with a transition to metallic behavior ( $\frac{\partial \rho}{\partial T} > 0$ ) occurring at  $p \approx 1.57 \times 10^{10} \text{ cm}^{-2}$ . With further increases in  $p$ , the metallic behavior weakens again, as expected because the hole-hole interactions weaken with increasing  $p$ . Very similar behavior is obtained in our device for  $d = 340$  nm, as shown in Fig. 2(b). At high densities, weak metallic behavior is observed, which becomes stronger as  $p$  is decreased. We are unable to measure in the insulating regime because our device becomes unstable when the top-gate bias is too high, however this is not an impediment to the experiments presented here.

In Fig. 3 we present  $\rho_{xx}(T)$  measured with  $d = 340$  nm (thick lines) and  $d = 50$  nm (thin lines) at five different densities deep in the metallic regime. Moving down through the panels in Fig. 3, the metallic behavior weakens with increasing  $p$ , as indicated by the percentage change in resistivity  $\Delta\rho$  over the measured temperature range. The most obvious effect of reducing  $d$  to 50 nm is to offset  $\rho_{xx}(T)$  to a lower resistivity, likely caused by the upper 2DHS screening the lower 2DHS from the long-range impurity scattering from the upper modulation doping layer.

The resistivity  $\rho_{xx}(T)$  is predominantly composed of three parts: a temperature-independent Drude contribu-

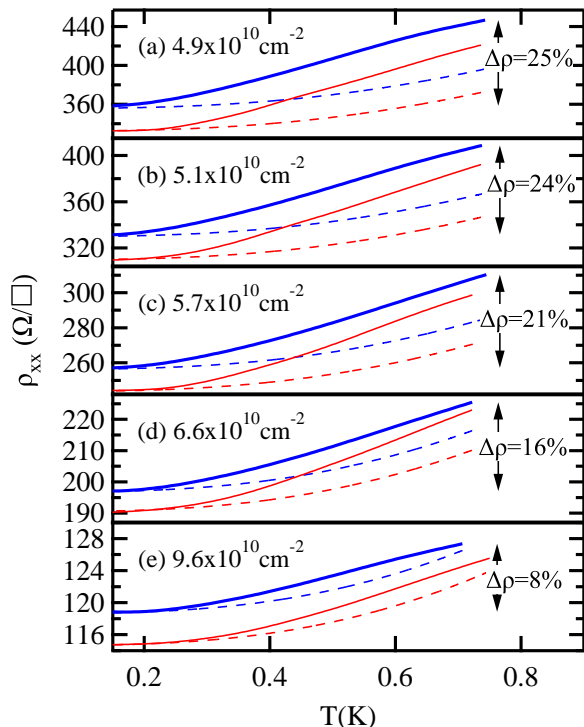


FIG. 3: (Color online) (a)-(e) The measured resistivity  $\rho_{xx}(T)$  vs temperature  $T$  for  $d = 50$  nm (thin red lines) and  $d = 340$  nm (thick blue lines) for five different densities  $p$ . The back-gate bias was the same for the two  $d$  values at each density. The dashed lines show the calculated phonon contributions (parameter free fits of Karpus' theory) in each case. The percentage change in resistivity from 150 mK to 0.7 K for  $d = 340$  nm is shown for each panel.

tion  $\rho_0$  due to impurity scattering, and two temperature-dependent contributions due to phonon scattering  $\rho_{ph}(T)$  and hole-hole interactions. We calculate  $\rho_{ph}(T)$  using Karpus' theory<sup>10</sup>, as done previously for 2D hole systems<sup>9,11</sup>. The Drude contribution  $\rho_0$  is then obtained by extrapolating  $\rho(T) - \rho_{ph}(T)$  to  $T = 0$ . The calculated phonon contributions for each  $d$  and  $p$  are presented as dashed lines in Fig. 3. At the highest density, where interactions are weakest,  $\rho_{ph}(T)$  is a remarkably good fit to the measured  $\rho(T)$  considering there are no fitting parameters, giving confidence in our application of Ref. 10 to calculating the phonon contribution. In contrast, at lower densities, there is a significant temperature dependence that cannot be described by phonon scattering alone, which we attribute to hole-hole interactions (screening).

Following Proskuryakov *et al.*, we isolate the contribution of the Coulomb interactions to the conductivity  $\sigma_{int}(T)$  by subtracting the phonon and Drude contributions using  $\sigma_{int}(T) = [\rho(T) - \rho_{ph}(T)]^{-1} - \rho_0^{-1}$ <sup>9</sup>. In Fig. 4 (a), we plot  $\sigma_{int}(T)$  vs  $T$  corresponding to the  $d = 50$  nm trace in Fig. 3(a), and find an approximately linear dependence of  $\sigma_{int}$  on  $T$ , with a negative slope corre-

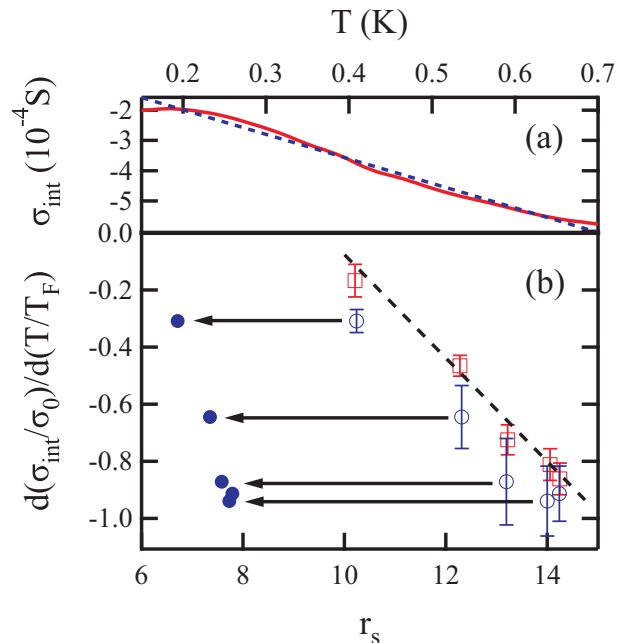


FIG. 4: (Color online) (a)  $\Delta\sigma$  vs  $T$  for  $p = 4.9 \times 10^{10} \text{ cm}^{-2}$  and  $d = 50$  nm. The data is the thin solid line and the linear fit is the thick dashed line. The error bars indicate the effect of varying the temperature range of the linear fits used to obtain  $d(\sigma_{int}/\sigma_0)/d(T/T_F)$ . Although the values change slightly, the observed trends are unaffected. (b) A plot of the metallicity  $d(\sigma_{int}/\sigma_0)/d(T/T_F)$  vs  $r_s$  for  $d = 340$  nm (open squares) and  $d = 50$  nm (open circles), and  $r_s^{dipole}$  for  $d = 50$  nm (closed circles). The dashed line is a guide to the eye for the trend exhibited by the  $d = 340$  nm data vs  $r_s^{bare}$  (open squares).

sponding to metallic behavior. It is common to interpret such data using the theory of Zala *et al.*<sup>7</sup> to obtain the Fermi liquid interaction parameter  $F_0^\sigma$ . This is normally achieved by fitting  $\sigma_{int}$  vs  $T$  in the linear regime (i.e.,  $T \ll T_F$ , where  $T_F$  is the Fermi temperature) to obtain the normalized slope  $d(\sigma_{int}/\sigma_0)/d(T/T_F)$ , which is related to  $F_0^\sigma$  by  $d(\sigma_{int}/\sigma_0)/d(T/T_F) = 1 + [3F_0^\sigma/(1 + F_0^\sigma)]$ <sup>12</sup>. However, recent studies have shown that the theory of Zala *et al.*<sup>7</sup>, which assumes a short-range scattering potential, does not extract the correct values of  $F_0^\sigma$  for modulation-doped samples where long-range scattering from remote ionized impurities is significant<sup>13</sup>. Hence in this paper, we focus on the slope  $d(\sigma_{int}/\sigma_0)/d(T/T_F)$  as a measure of the strength of the metallic behavior, henceforth called the 'metallicity', and simply note that if we fit Zala's theory to our data, we obtain  $F_0^\sigma$  values similar to those previously obtained in modulation-doped GaAs 2D hole systems by Proskuryakov *et al.*<sup>9</sup>.

We now directly analyze the effect of changing the ground-plane separation  $d$ , and thus the length-scale of the Coulomb interactions, on the metallic behavior. To do this, we obtain the metallicity  $d(\sigma_{int}/\sigma_0)/d(T/T_F)$  for each trace in Fig. 3 by taking a linear fit to the corresponding  $\sigma_{int}$  vs  $T$  data (Fig. 4(a)). We limit our fitting to the range  $150 \text{ mK} < T < 0.7 \text{ K}$ . The

lower limit is the minimum hole temperature in our experiment (obtained following<sup>14</sup>) whilst the upper limit ensures that  $T \ll T_F$ . The relative strength of the hole-hole Coulomb interactions is characterized by  $r_s$ , which in the absence of a nearby ground-plane, takes the form  $r_s^{bare} = (m^*e^2)/(4\pi^{3/2}\hbar^2\epsilon\sqrt{p})$ , where  $\epsilon$  is the dielectric constant. In Fig. 4(b), we plot the metallicity  $d(\sigma_{int}/\sigma_0)/d(T/T_F)$  as a function of  $r_s^{bare}$  for  $d = 340$  nm (open squares) and  $d = 50$  nm (open circles). In each case  $d(\sigma_{int}/\sigma_0)/d(T/T_F)$  is negative, indicating metallic behavior. As Fig. 4(b) shows, there is little change in the metallicity as  $d$  is reduced from 340 nm to 50 nm at constant density, but the metallic behavior weakens with increasing density (i.e., decreasing  $r_s$ ), as expected. The presence of the ground-plane introduces negative image-charges that cause the holes to interact as though they were dipoles rather than single positive charges, resulting in a Coulomb potential that falls off as  $\sim 1/r^3$  instead of  $1/r$  for  $r \geq 2d^4$ . This leads to an additional term in  $r_s$  that accounts for the Coulomb interaction between the hole's image-charge and another hole in the 2DHS, giving<sup>15,16</sup>:

$$r_s^{dipole} = \frac{m^*e^2}{4\pi^2\hbar^2\epsilon p} [(\pi p)^{1/2} - (\frac{1}{\pi p} + d^2)^{-1/2}]$$

The additional term in Eqn (1) reduces the effective  $r_s$  as  $d$  becomes comparable to the hole-hole separation<sup>4</sup>  $a = 2(\pi p)^{1/2}$ , with  $a$  ranging from 36 – 51 nm for the data in Fig. 3. Thus, whilst for  $d = 340$  nm the effective reduction in  $r_s$  is quite small ( $< 8\%$ ), it is quite substantial for  $d = 50$  nm, as demonstrated in Fig. 4(b), where we have re-plotted the metallicity for  $d = 50$  nm vs.  $r_s^{dipole}$  (solid circles).

We now consider the effect of the ground plane on the metallicity. The dashed line in Fig. 4(b) shows the metallicity of the unscreened  $d = 340$  nm data tends to decrease as  $r_s$  is reduced. If the metallicity depends only on  $r_s$ , for example, if it is due to long-range Coulomb interactions<sup>7</sup>, then when the effective  $r_s$  is decreased by reducing  $d$  from 340 nm to 50 nm, the metallicity should also be reduced. When plotted against  $r_s^{dipole}$ , the metallicity for the  $d = 50$  nm data (solid circles) should lie in the upper left corner of Fig. 4(b), not down in the lower left of the figure. In fact rather than being reduced, the  $d = 50$  nm metallicity is actually slightly greater than for  $d = 340$  nm, suggesting that the ground-plane has almost no effect on the metallic behavior. This is in con-

trast to recent experiments on the screening of long-range Coulomb interactions in the insulating regime<sup>4</sup>, where single layer 2DHS samples with  $d = 250, 500$  and  $600$  nm were examined. The hopping conductivity was fitted to the form  $\sigma/(e^2/h) = G_0 + (T/T_0)^\alpha$ , and the exponent  $\alpha$ , which is related to the strength of the insulating behavior, was found to be very sensitive to  $d$ , and uniquely determined by the ratio  $d/a$ , which was changed from 1.1 to 5 [4]. In our experiment,  $d/a$  changes by almost an order of magnitude, from 2 to 19, yet we find that the metallicity is primarily determined by  $a$  alone.

One possible explanation for the contrasting behaviour is that in the metallic regime the long-range Coulomb interactions are already screened by the other holes in the 2DHS, significantly diminishing the effect of the ground-plane. In the insulating regime, this screening by other holes is much weaker, giving the ground-plane significant effect. This is consistent with recent studies of the compressibility of 2D systems<sup>18</sup>, which found that the Thomas-Fermi screening radius increases by over an order of magnitude when going from the metallic to insulating regime.

We finish with some final comments on the experiment. First, it is particularly interesting to note that our findings are consistent with the metallic behavior being due to the temperature-dependent screening of the hole-impurity Coulomb interactions<sup>5,6,7</sup>. Second, because the screening layer for  $d = 50$  nm is a nearby 2DHS, we have estimated the possible contribution of Coulomb drag to  $\Delta\rho(T)$ , since this can be a significant effect in DQW structures<sup>17</sup>. Due to the relatively large QW spacing and high densities, we calculate the drag contribution to  $\Delta\rho(T)$  to be  $< 1\%$  in our device. Finally, in addition to theoretical calculations<sup>16</sup>, we have performed experiments to check that the upper 2DHS density is sufficient to act as a proper screening layer. We find no change in the metallic behavior when the upper 2DHS density is varied<sup>19</sup>, confirming that the upper 2DHS acts as an effective ground-plane.

This work was funded by Australian Research Council (ARC) and the EPSRC. L.H.H. acknowledges support from the UNSW and the CSIRO. O.K. acknowledges support from the UNSW. M.Y.S, A.R.H, A.P.M. and R.D. acknowledge support from the ARC. We thank O.P. Sushkov for helpful discussions and J. Cochrane for technical support.

\* Electronic address: laphang@phys.unsw.edu.au

† Present Address: Low Temperature Laboratory, Helsinki University of Technology, PO Box 3500, 02015 TKK, Finland

‡ Electronic address: Alex.Hamilton@unsw.edu.au

<sup>1</sup> B.L. Altshuler, D.L. Maslov and V.M. Pudalov, *Physica E* **9**, 2, (2001); S. V. Kravchenko and M. P. Sarachik, *Rep.*

*Prog. Phys.*, **67**, 1, (2004)

<sup>2</sup> H.-W. Jiang and A. J. Dahm, *Surf. Sci.* **196**, 1 (1988).

<sup>3</sup> G. Mistura, T. Günzler, S. Nesper, and P. Leiderer, *Phys. Rev. B* **56**, 8360 (1997).

<sup>4</sup> J. Huang, D. S. Novikov, D. C. Tsui, L. N. Pfeiffer and K. W. West, *cond-mat/0610320*.

<sup>5</sup> A. Gold, *Phys. Rev. B* **41**, 8537 (1990).

- <sup>6</sup> S. Das Sarma and E.H. Hwang, Phys. Rev. B **61**, R7838 (2000).
- <sup>7</sup> G. Zala, B. N. Narozhny, and I.L. Aleiner, Phys. Rev. B **64**, 214204 (2001).
- <sup>8</sup> A. R. Hamilton, M. Y. Simmons, M. Pepper, E. H. Linfield, and D. A. Ritchie, Phys. Rev. Lett. **87**, 126802 (2001).
- <sup>9</sup> Y. Y. Proskuryakov, A. K. Savchenko, S. S. Safonov, M. Pepper, M. Y. Simmons, and D. A. Ritchie, Phys. Rev. Lett. **89**, 076406 (2002).
- <sup>10</sup> V. Karpus, Semicond. Sci. Tech. **5**, 691 (1990).
- <sup>11</sup> C. E. Yasin, T. L. Sobey, A. P. Micolich, A. R. Hamilton, M. Y. Simmons, W. R. Clarke, L. N. Pfeiffer, K. W. West, E. H. Linfield, M. Pepper, and D. A. Ritchie, Phys. Rev. B **72**, 241310(R) (2005).
- <sup>12</sup> H. Noh, M. P. Lilly, D. C. Tsui, J. A. Simmons, E. H. Hwang, S. Das Sarma, L. N. Pfeiffer, and K. W. West, Phys. Rev. B **68**, 165308 (2003).
- <sup>13</sup> W. R. Clarke, C. E. Yasin, A. R. Hamilton, A. P. Micolich, M. Y. Simmons, K. Muraki, Y. Hirayama, M. Pepper and D. A. Ritchie, Nature Physics **4**, 55 (2008).
- <sup>14</sup> S. McPhail, C.E. Yasin, A.R. Hamilton, M.Y. Simmons, E.H. Linfield, M. Pepper and D.A. Ritchie, Phys. Rev. B **70**, 245311 (2004).
- <sup>15</sup> A. Widom and R. Tao, Phys. Rev. B **38**, 10787 (1988).
- <sup>16</sup> O.P. Sushkov (Private Communication); calculations showing that the 2DHS produces almost exactly the same effect as a metal gate will be published elsewhere.
- <sup>17</sup> R. Pillarisetty, H. Noh, E. Tutuc, E. P. De Poortere, K. Lai, D. C. Tsui and M. Shayegan, Phys. Rev. B **71**, 115307 (2005).
- <sup>18</sup> G. Allison, E. A. Galaktionov, A. K. Savchenko, S. S. Safonov, M. M. Fogler, M. Y. Simmons, and D. A. Ritchie, Phys. Rev. Lett. **96**, 216407 (2006).
- <sup>19</sup> L.H. Ho, W.R. Clarke, R. Danneau, O. Klochan, A.P. Micolich, M.Y. Simmons, A.R. Hamilton, M. Pepper and D.A. Ritchie, Physica E **40**, 1700 (2008)